

# Optimal phase shift design for fair allocation in RIS aided uplink network using statistical CSI

Athira Subhash, Abla Kammoun, Ahmed Elzanaty, Sheetal Kalyani, Yazan H. Al-Badarneh, and Mohamed-Slim Alouini

## Abstract

Reconfigurable intelligent surface (RIS) can be crucial in next-generation communication systems. However, designing the RIS phases according to the instantaneous channel state information (CSI) can be challenging in practice due to the short coherent time of the channel. In this regard, we propose a novel algorithm based on the channel statistics of massive multiple input multiple output systems rather than the CSI. The beamforming at the base station (BS), power allocation of the users, and phase shifts at the RIS elements are optimized to maximize the minimum signal to interference and noise ratio (SINR), guaranteeing fair operation among various users. In particular, we design the RIS phases by leveraging the asymptotic deterministic equivalent of the minimum SINR that depends only on the channel statistics. This significantly reduces the computational complexity and the amount of controlling data between the BS and RIS for updating the phases. This setup is also useful for electromagnetic fields (EMF)-aware systems with constraints on the maximum user's exposure to EMF. The numerical results show that the proposed algorithms achieve more than 100% gain in terms of minimum SINR, compared to a system with random RIS phase shifts, with 40 RIS elements, 20 antennas at the BS and 10 users, respectively.

## Index Terms

A. Subhash, and S. Kalyani are with the Department of Electrical Engineering, Indian Institute of Technology, Madras, India. (email: {ee16d027@smail,skalyani@ee}.iitm.ac.in).

A. Elzanaty is with the 5GIC & 6GIC, Institute for Communication Systems (ICS), University of Surrey, Guildford, GU2 7XH, United Kingdom (e-mail: a.elzanaty@surrey.ac.uk)

Y. H. Al-Badarneh is with the Department of Electrical Engineering, The University of Jordan, Amman, 11942 (email: yalbadarneh@ju.edu.jo).

A. Kammoun and M.-S. Alouini are with the Computer Electrical and Mathematical Sciences and Engineering (CEMSE) Division, King Abdullah University of Science and Technology (KAUST), Thuwal, Makkah Province, Saudi Arabia. (e-mail: {abla.kammoun,slim.alouini}@kaust.edu.sa).

Reconfigurable Intelligent Surface; statistical channel state information; electromagnetic fields (EMF)-aware design

## I. INTRODUCTION

The idea of reconfigurable intelligent surfaces (RIS) capable of reconfiguring the wireless propagation environment has recently attracted much research attention [1], [2]. RISs, also widely referred to as intelligent reflecting surfaces (IRS), are surfaces made of metamaterials capable of modifying the properties of electromagnetic radiation impinging them according to some control mechanisms [3]. The modified properties may include the amplitude, phase, frequency or polarization of the impinging wave. The most commonly studied RIS model is the one changing the phase of the incident wave [1]. RIS usually comprises an array of reflecting elements, each capable of individually modifying the properties of the incident wave and the associated control mechanism. Note that such a structure can modify the wireless propagation environment and hence can be used to achieve beam-steering and focusing [3]. Therefore RIS is a potential enabler for the concept of smart radio environments. Conventionally, improvements in wireless system performance were achieved by improving the transmitter and receiver design to combat the detrimental effects of the wireless propagation channel. Smart radio environments aim to introduce controlled changes in the wireless channel to improve signal propagation [3], [4] and a RIS proves to be one enabler for the same.

Several works in the literature have studied the prospects of potential improvements in the wireless system performance by deploying RIS to improve cell coverage, compensate for the absence of a line of sight (LOS) link, enhance the physical layer security, in millimetre (mm) wave channels and several other applications [5]–[8]. The authors of [6] study the channel capacity optimization of single-stream transmission using RISs in a mmWave system without any LOS path. They propose a scheme to optimize the RIS phase shifts and the transmit phase precoder to maximize the capacity. The authors of [9] maximize the weighted sum rate of the users by jointly designing the beamforming (BF) at the access point and the phase shifts of the RIS elements in a downlink multiple input single output (MISO) system. The authors of [10] propose a joint optimization strategy to select the optimal beamformer at the access point (AP) and the RIS phase shifts to maximize the spectral efficiency (SE) in the downlink of a single user MISO system. A deep reinforcement-based resource allocation is proposed for a single-user MISO system by the authors of [11]. The downlink multi-user MISO systems are considered by

the authors of [12], [13]. An algorithm to find the optimal BF strategy and phase shift design that minimizes transmit power at the AP, subject to constraints on the signal to interference and noise ratio (SINR) of each user, is proposed in [13]. The authors of [14] study the resource allocation in a RIS aided spatially modulated multiple input multiple output (MIMO) uplink network. They propose an algorithm for the joint optimization of the users' transmit power and the RIS phase shifts to minimize the system symbol error. A fair resource allocation strategy to maximize the minimum SINR is discussed in [12]. They also study the susceptibility of the system to channel estimation errors.

In all of the above works, the availability of exact channel state information (CSI) at all the nodes is assumed. Note that this assumption might not be practical in all scenarios. Moreover, given the time-varying nature of the wireless channel, resource allocation strategies using the exact CSI will be valid only over the coherence time and must be updated frequently. This would, in turn, increase the computational complexity and the feedback overhead, especially in updating the RIS phase shifts. Using statistical CSI can significantly reduce the channel estimation overhead and computational complexity in such scenarios [15]. Several authors have explored the prospects of using statistical CSI for resource allocation problems in RIS-aided systems.

A single-user MIMO system assisted by a RIS is studied by the authors of [16]. Assuming that the statistical CSI is known at both the transmitter and the RIS, they propose a resource allocation scheme to maximize the ergodic SE. An upper bound on the SE is derived and utilized to develop the resource allocation strategy. The authors of [17] propose a strategy for designing the transmit covariance matrices of the users and the RIS phase shift matrix to maximize the system global energy efficiency (GEE) with partial CSI assuming the correlated Rayleigh model. Using results from random matrix theory (RMT), asymptotic deterministic equivalents of the GEE are first derived and then used to solve the optimization problem. The authors of [18] study the outage performance of RIS-aided MIMO communications over cascaded Rayleigh fading channels. A genetic algorithm is used to find the optimal phase shift design that minimizes the asymptotic outage probability. The outage probability at the destination of a RIS-assisted communication system in a  $\kappa - \mu$  fading environment is studied by the authors of [19]. The downlink of a multi-user MISO system is studied by the authors of [20]. They solve the problem of determining the optimal linear precoder, the power allocation matrix at the BS and the RIS phase shifts matrix to maximize the system's minimum SINR. Assuming a full-rank BS-to-RIS channel matrix results

from RMT are used to derive deterministic approximations for the minimum user SINR. This is, in turn, used to propose the optimal phase shift design algorithm. Similarly, the downlink of a multi-user MIMO system supported by a RIS is studied by the authors of [21]. They propose an optimization algorithm to configure the RISs to maximize the network sum rate. The proposed solution depends only on the distribution of the users' locations and the distribution of the multipath channel, hence avoiding the need for frequently reconfiguring the RIS. A brief overview of the differences in the models studied in a few of the key literature discussed above is presented in Table I.

To the best of our knowledge, the interesting scenario of fair resource allocation in a RIS-aided uplink network with constraints on the per-user transmit power has not been studied in literature so far. Such a fair resource allocation scheme will be of interest in several multi-user scenarios. Moreover, a resource allocation strategy that does not need to be repeated for every channel realization will be of utility in any practical scenario. Since the RIS phase shift design is usually evaluated at some access point and later fed back to the RIS controller, a RIS phase shift design depending on the exact channel statistics will lead to a large feedback overhead. Hence, it is of particular interest to explore a solution for the optimal RIS phase, which will depend only on the channel statistics. Such a solution will be valid for a longer time and considerably reduce the feedback overheads.

In this regard, we consider the uplink communication of a multi-user single input multiple output (SIMO) system assisted by a multi-element RIS with correlated elements. We study the joint optimization of the receive BF vectors at the BS, transmit power at the users and the phase shift vector at the RIS that maximizes the minimum SINR. An alternating optimization strategy is proposed to solve the joint resource allocation problem. The BF vector design and the transmit power allocation assume the availability of the exact CSI and are implemented using the results from [22]. To simplify the computational complexity and to avoid frequent feedback, the phase shift at the RIS is designed using the statistical CSI only. More elaborately, we use tools from RMT to derive the asymptotic deterministic equivalent of the minimum user SINR for the large system dimensions. Later, the phase shift optimization is performed using this deterministic equivalent. We also demonstrate the utility of the proposed results for the joint resource allocation of RIS-aided communication systems with constraints in the maximum electromagnetic field (EMF) exposure.

Recently, the EMF exposure of the users has been a concern in the fifth-generation commu-

nication systems [23]. There has been an increase in the number of users concerned about the effects of continued exposure to EMFs, and hence there are many recent literatures studying this problem in detail [23]–[26]. The authors of [23] discuss the health effects of EMF exposure, metrics to characterize the exposure and a review of the different approaches targeted to reduce the exposure in 5G systems. A survey on EMF exposure and a discussion on possible techniques for reducing EM radiation exposure in mobile communication systems using concepts related to specific absorption rate (SAR) and transmit power reduction in mobile systems is available in [24]. The SAR (measured in Watts per kilogramme of body weight (W/kg)) measures the EM radiation exposure level in the near-field region. It measures the rate of energy absorption by the body when exposed to EM radiation. EM exposure from mobile phones is mostly in the near-field, so SAR is used to evaluate such exposure over a certain period of time [24]. The authors of [25] propose a technique for evaluating and optimizing the SAR for multi-antenna wireless systems. The problem of optimal resource allocation that minimizes EMF of users while maintaining the quality of service (QoS) requirements has received much attention recently [27], [28]. The authors of [28] propose a scheme to minimize the human exposure to EMF radiations while achieving the target throughput using probabilistic shaping. The EMF exposure in RIS-aided communication systems is studied in [27]. They propose an optimization strategy to select the RIS phases to minimize the EMF exposure in terms of the exposure index while maintaining a minimum target QoS for the users. The authors of [29] propose an optimization strategy to minimize the average exposure dose of users, considering both the system's QoS and transmit power constraints. Given that our resource allocation scheme maximizes the minimum user SINR, we must ensure that the resulting solution will not result in users experiencing more EMF radiation than the stipulated thresholds. Hence, we demonstrate how the problem can be studied with constraints imposed on the maximum EMF exposure of each user. The main contributions of this paper can be summarized as follows:

- We formulate the problem of jointly optimizing the receive BF vectors at the BS, transmit power allocation at the users, and the RIS phase shift design in a RIS-aided multi-user system with multiple antennas at the BS. We discuss solutions for the BF and power allocation, assuming the availability of exact CSI.
- We then study the asymptotic statistics of the minimum SINR for this BF choice at the BS. We use tools from RMT to derive the asymptotic deterministic equivalent of received

Reference	Instantaneous CSI/ Statistical CSI	Objective	Uplink/ Downlink	Antenna model
[10]	Instantaneous	SE	Downlink	MISO
[11]	Instantaneous	Received SNR	Downlink	MISO
[13]	Instantaneous	Achievable rate	Downlink	MISO
[15]	Statistical	Ergodic rate	Uplink	MIMO
[16]	Statistics	Ergodic spectral efficiency	Uplink	MIMO
[17]	Partial	Energy efficiency	Uplink	MIMO
[20]	Instantaneous	Minimum SINR	Downlink	MISO
[14]	Instantaneous	Symbol error rate	Uplink	MIMO
[22]	Instantaneous	Minimum SINR	Uplink	SIMO
This work	Statistical	Minimum SINR	Uplink	SIMO

TABLE I: Key literature studying RIS phase optimization.

SINR.

- A simple projected gradient descent-based solution is proposed to identify the optimal phase shift choice at the RIS that maximizes the asymptotic minimum user SINR.
- This solution has less computational complexity and depends on large-scale channel gains. Thus, the proposed scheme also avoids the need for frequent reconfiguration of the RIS with costly feedback.

The rest of the paper is organized as follows. Section II presents the system model, Section III explains the proposed optimization problem and the corresponding solution. Section IV discusses one application for the proposed results, and Section V demonstrates the results of simulation experiments. Finally, we conclude the work in Section VI

## II. SYSTEM MODEL

We consider the uplink communication of a multi-user SIMO system where  $K$  single antenna users communicate to an  $M$ -antenna BS with the help of an  $N$  element RIS array. The signal received at the BS is given by

$$\mathbf{y} = \left( \mathbf{H}_1 \mathbf{R}_{\text{RIS}}^{\frac{1}{2}} \boldsymbol{\Phi} \mathbf{H}_2 \right) \mathbf{x} + \mathbf{n}, \quad (1)$$

where  $\mathbf{H}_1 \in \mathbb{C}^{M \times N}$  represents the LOS channel matrix between the BS and RIS,  $\mathbf{R}_{\text{RIS}} \in \mathbb{C}^{N \times N}$  represents the spatial correlation matrix of the RIS elements,  $\mathbf{H}_2 \in \mathbb{C}^{N \times K}$  represents the channel between the  $K$  users and the RIS, i.e  $\mathbf{h}_{2,k} = \ell_k \tilde{\mathbf{h}}_{2,k}$  where  $\ell_k$  is the path loss corresponding to the link between user  $k$  and the RIS and  $\tilde{\mathbf{h}}_{2,k} \sim \mathcal{CN}(\mathbf{0}, \mathbf{I}_N) \in \mathbb{C}^{N \times 1}$  denotes the fading channel gain between the RIS and user  $k$ ,  $\mathbf{x}$  represents the transmit signal vector and  $n_k$

represents the thermal noise, modeled as a  $\mathcal{CN}(0, \tilde{\sigma}^2)$  random variable (RV). Furthermore, we have  $\Phi = \text{diag}(\phi_1, \dots, \phi_N) \in \mathbb{C}^{N \times N}$  is the diagonal matrix accounting for the response of the RIS elements, and  $\phi_n = \exp(j\theta_n)$ ,  $n \in \{1, \dots, N\}$ , where  $\theta_n$  is the phase shift induced by the  $n$ -th RIS element. Note that the received signal can be rewritten as

$$\mathbf{y} = \sum_{k=1}^K p_k \mathbf{H}_1 \mathbf{R}_{\text{RIS}}^{\frac{1}{2}} \Phi \mathbf{h}_{2,k} x_k + \mathbf{n}, \quad (2)$$

where  $x_k$  represents the complex symbol transmitted from user  $k$  with transmit power  $p_k$ . Now, let  $\boldsymbol{\beta} \in \mathbb{C}^{K \times M}$  be the BF matrix at the BS, and the received symbols can be decoded as

$$\mathbf{r} = \boldsymbol{\beta} \mathbf{y}. \quad (3)$$

Then, the decoded symbol from user  $k$  can be represented as

$$r_k = \boldsymbol{\beta}_k^H \mathbf{y}, \quad (4)$$

where  $\boldsymbol{\beta}_k$  is the  $k$ -th row of the matrix  $\boldsymbol{\beta}$ . The SINR for user  $k$  at the BS is hence given by

$$\text{SINR}_k = \frac{\frac{p_k}{K} \left| \boldsymbol{\beta}_k^H \mathbf{H}_1 \mathbf{R}_{\text{RIS}}^{\frac{1}{2}} \Phi \mathbf{h}_{2,k} \right|^2}{\sum_{i=1, i \neq k}^K \frac{p_i}{K} \left| \boldsymbol{\beta}_k^H \mathbf{H}_1 \mathbf{R}_{\text{RIS}}^{\frac{1}{2}} \Phi \mathbf{h}_{2,i} \right|^2 + \sigma^2 \|\boldsymbol{\beta}_k\|^2}, \quad (5)$$

where  $\sigma^2 = \frac{\tilde{\sigma}^2}{K}$ . The SINR experienced by each user is thus a function of the power allocation, BF at the BS, and the phase shift induced by the RIS elements. To ensure a fair service for all users, we would like to jointly optimize these variables such that the minimum SINR in the system is maximized, i.e., maximizing  $\min_{k \in \mathcal{K}} \text{SINR}_k$ . In the next section, we formulate an optimization problem to identify the optimal power allocation vector, BF vectors at the BS and phase shifts introduced by the IRS elements such that the constraints on the transmit power of each user are satisfied. We also discuss how the studied optimization problem can be used for the resource allocation of RIS-aided communication systems with constraints on the maximum EMF of each user.

### III. OPTIMIZATION PROBLEM AND SOLUTION

The optimization problem discussed in the last section can be mathematically formulated as follows:

$$\begin{aligned}
 & \max_{\{p_k\}, \Phi, \beta} \quad \min_k \text{SINR}_k \\
 \text{s.t.} \quad & 0 \leq \frac{p_k}{K} \leq p_{\max,k}; \quad \forall k \in \{1, \dots, K\}, \\
 & \|\beta_k\| = 1; \quad \forall k \in \{1, \dots, K\}, \\
 & |\phi_n| = 1, \quad \forall n \in \{1, \dots, N\}.
 \end{aligned} \tag{\mathcal{P}_1}$$

Note that we have also imposed constraints on the norm of each BF vector and the magnitudes of the phase shift at each of the RIS elements. The solution for the above optimization problem depends upon the instantaneous channel gains, and hence the BF, power allocation vector, and phase shift vector at the RIS need to be updated for every different channel realization, i.e., after the channel coherence time. Hence, the optimal RIS phase shift needs to be evaluated at the BS for every channel realization, and there needs to be a feedback scheme to send this information to the RIS. Such frequent feedbacks are costly, and hence in this work, we propose to design the phase shift vector at the RIS using statistical CSI. Note that the joint optimization of the BF matrix, the power variables and the RIS phase shift vector is not a convex problem and hence does not admit a very simple solution. We propose using the simple alternating optimization technique wherein the joint optimization problem is broken down into multiple sub-problems, which are solved independently. We shall then iterate over the solutions for each problem until the solution converges. For BF and power allocation, we follow the same approach as [22], and the corresponding solutions are discussed in the next paragraph.

#### A. BF and power allocation

The optimal BF vector is given by the solution for the following problem:

$$\begin{aligned}
 & \max_{\beta} \quad \min_k \text{SINR}_k \\
 \text{s.t.} \quad & \|\beta_k\| = 1; \quad \forall k \in \{1, \dots, K\}.
 \end{aligned} \tag{\mathcal{SP}_1}$$

Following the steps in [22], the solution for the above problem is given by,

$$\beta_k = \frac{(\Sigma_k + \sigma^2 \mathbf{I})^{-1} \mathbf{g}_k}{\|(\Sigma_k + \sigma^2 \mathbf{I})^{-1} \mathbf{g}_k\|}, \tag{6}$$

where  $\Sigma_k = \sum_{i=1, i \neq k}^K \frac{p_i}{K} \mathbf{g}_i \mathbf{g}_i^H$  and  $\mathbf{g}_k = \mathbf{H}_1 \mathbf{R}_{\text{RIS}}^{\frac{1}{2}} \Phi \mathbf{h}_{2,k}$ . For this choice of  $\{\beta_k\}$ , the SINR of the  $k$ -th user is given by,

$$\text{SINR}_k = \frac{p_k}{K} \mathbf{g}_k^H (\Sigma_k + \sigma^2 \mathbf{I})^{-1} \mathbf{g}_k. \quad (7)$$

Similarly, the sub-problem of identifying the optimal transmit power policy can be formulated as follows,

$$\begin{aligned} \max_{\{p_k\}} \quad & \min_k \text{SINR}_k \\ \text{s.t.} \quad & 0 \leq \frac{p_k}{K} \leq p_{\max,k}; \quad \forall k \in \{1, \dots, K\}. \end{aligned} \quad (8)$$

Following steps similar to [30, Eqn.(2)], this problem can be rewritten as

$$\begin{aligned} \min_{\{p_k\}, \tau} \quad & \tau^{-1} \\ \text{s.t.} \quad & \frac{\tau \left( \sum_{i=1, i \neq k}^K \frac{p_i}{K} f_{k,i} + n_k \right)}{p_k f_{k,k}} \leq 1 \quad \forall k \in \{1, \dots, K\}, \\ & 0 \leq \frac{p_k}{K} \leq p_{\max,k} \quad \forall k \in \{1, \dots, K\}, \end{aligned} \quad (\mathcal{SP}_2)$$

where  $f_{k,i} = \left| \beta_k^H \mathbf{H}_1 \mathbf{R}_{\text{RIS}}^{\frac{1}{2}} \Phi \mathbf{h}_{2,i} \right|^2$  and  $n_k = \sigma^2$ . The above problem can be solved using the popular technique of geometric programming. Geometric programming solvers are available in popular optimization packages like CVX and can be solved efficiently [31].

### B. Phase shift design using asymptotic statistics

In this section, we study a phase shift design strategy using the deterministic equivalent of the minimum SINR instead of the exact expression for the minimum. We study the following two approaches here:

1. *Approach 1*: BS has full CSI and performs the BF optimization, and both power allocation and IRS phase shift design are performed using statistical CSI.
2. *Approach 2*: BF and power allocation are performed using exact CSI, and only phase shift design is performed using statistical CSI.

To set the stage for both designs, we will carry out an asymptotic analysis of the users' SINR and their allocated powers. Now, using the optimal BF vectors in (6), the power allocation is achieved by solving the optimization problem in  $\mathcal{P}_2$ . In [32], the authors addressed a similar

problem to study max-min fairness optimization in wireless networks. Using Lemma 1 from [32], we observe that the optimal solution for  $\mathcal{P}_2$  would ensure that all the users experience the same SINR, say  $\tau^*$ . Thus, we have,

$$\tau^* = \text{SINR}_k = \frac{p_k^*}{K} \mathbf{g}_k^H (\Sigma_k + \sigma^2 \mathbf{I})^{-1} \mathbf{g}_k \quad \forall k \in \{1, \dots, K\}. \quad (9)$$

Let us rewrite  $\tau^*$  as  $\tau^* = \frac{p_k^*}{K} \ell_k \tilde{\mathbf{g}}_k^H (\Sigma_k + \sigma^2 \mathbf{I})^{-1} \tilde{\mathbf{g}}_k$ , where  $\tilde{\mathbf{g}}_k = \underbrace{\mathbf{H}_1 \mathbf{R}_{\text{RIS}}^{\frac{1}{2}} \Phi \mathbf{R}_{\text{users}}^{\frac{1}{2}} \tilde{\mathbf{h}}_{2,k}}_{\mathbf{U}}$  and  $\mathbf{g}_k = \sqrt{\ell_k} \tilde{\mathbf{g}}_k$ . Letting  $d_k := \frac{1}{K} \tilde{\mathbf{g}}_k^H (\Sigma_k + \sigma^2 \mathbf{I})^{-1} \tilde{\mathbf{g}}_k = \frac{1}{K} \tilde{\mathbf{h}}_{2,k}^H \mathbf{U}^H (\Sigma_k + \sigma^2 \mathbf{I})^{-1} \mathbf{U} \tilde{\mathbf{h}}_{2,k}$ , we obtain

$$\tau^* = p_k^* \ell_k d_k \quad (10)$$

or equivalently  $p_k^* = \frac{\tau^*}{\ell_k d_k}$ .

Using (10), we can see that  $d_1, \dots, d_K$  are solutions to the following system of equations:

$$d_k = h_k(d_1, \dots, d_K; \tau^*), \quad k = 1, \dots, K \quad (11)$$

where  $h_k(d_1, \dots, d_K; \tau) : \mathbb{R}^K \times \mathbb{R} : (d_1, \dots, d_K) \mapsto \frac{1}{K} \tilde{\mathbf{g}}_k^H \left( \sum_{i \neq k} \frac{\tau}{d_i} \tilde{\mathbf{g}}_i \tilde{\mathbf{g}}_i^H + \sigma^2 \mathbf{I} \right)^{-1} \tilde{\mathbf{g}}_k$ . To continue, we exploit the fact that  $h : \mathbb{R}^K \rightarrow \mathbb{R}^K : (d_1, \dots, d_K) \mapsto h_k(d_1, \dots, d_K; \tau)$  is a standard interference function. Hence, existence and uniqueness of the solution to (11) hold true for any  $\tau \geq 0$ . Particularly, letting  $\tau \geq 0$ , the following system of equations:

$$d_k = h_k(d_1, \dots, d_K; \tau), \quad k = 1, \dots, K \quad (12)$$

admits a unique solution which we denote by  $d_1(\tau), \dots, d_K(\tau)$ . With this, we may prove that  $\mathcal{P}_2$  amounts to solving the following problem:

$$\min_{d_k, \tau} \frac{1}{\tau} \quad (\mathcal{P}_{\text{eq}})$$

$$\text{s.t.} \quad d_k(\tau) = h_k(d_1, \dots, d_K; \tau), \quad k = 1, \dots, K \quad (13)$$

$$\frac{\tau}{d_k(\tau)} \leq K \ell_k p_{\max, k}, \quad k = 1, \dots, K. \quad (14)$$

The equivalent problem  $\mathcal{P}_{\text{eq}}$  is not convex. However, when it comes to asymptotic analysis, it is much simpler to handle. Prior to stating our main results, we shall first introduce the growth rate regime considered in our asymptotic analysis. Particularly, we will assume the following Assumptions:

*Assumption 1:*  $M, N$  and  $K$  grow large with a bounded ratio as  $0 < \liminf \frac{K}{M} \leq \limsup \frac{K}{M} < 1$  and  $0 < \liminf \frac{N}{M} \leq \limsup \frac{N}{M} < \infty$ . In the sequel, this assumption is denoted as  $\xrightarrow[M \rightarrow \infty]$ .

*Assumption 2:* The sequence of correlation matrices  $(\mathbf{R}_{\text{RIS}})_N$ ,  $(\mathbf{R}_{\text{users}})_N$  and the channel matrices  $(\mathbf{H}_1)_M$  satisfy:

$$\limsup_{M,N,K} \max(\|\mathbf{R}_{\text{RIS}}\|, \|\mathbf{R}_{\text{users}}\|, \|\mathbf{H}_1\|) < \infty.$$

Moreover, the sequence of maximum powers  $p_{\max,k}$  and link path losses  $\ell_k$ ,  $k = 1, \dots, K$  satisfy

$$\limsup_{M,N,K} \max_{1 \leq k \leq K} K \ell_k p_{\max,k} < \infty.$$

and

$$\liminf_{M,N,K} \max_{1 \leq k \leq K} K \ell_k p_{\max,k} > 0.$$

**Theorem 1.** Consider the regime in Assumption 1 and Assumption 2. For  $\tau \geq 0$ , let  $d_1(\tau), \dots, d_K(\tau)$  be the unique solutions to (12). Then, the following equation:

$$d = \frac{1}{K} \text{Trace} \left\{ \mathbf{U} \mathbf{U}^H \left( \mathbf{U} \mathbf{U}^H \frac{\tau}{d(1+\tau)} + \sigma^2 \mathbf{I} \right)^{-1} \right\}$$

admits a unique solution  $\bar{d}(\tau)$ . Moreover, for any compact interval  $\mathcal{I} \subset (0, \infty)$ , we have:

$$0 < \inf_{\tau \in \mathcal{I}} \bar{d}(\tau) \leq \sup_{\tau \in \mathcal{I}} \bar{d}(\tau) < \infty$$

and

$$\sup_{\tau \in \mathcal{I}} \max_{1 \leq k \leq K} |d_k(\tau) - \bar{d}(\tau)| \xrightarrow{M \rightarrow \infty} 0.$$

*Proof.* The proof of Theorem 1 is deferred to Appendix B. □

Theorem 1 studies the asymptotic behaviour of fixed point equations of standard interference functions in the form of (12). We believe that it can be used beyond the context of our work to handle, for instance, constraints expressed as linear combinations of user powers. For this reason, we formulate it as a stand-alone result to facilitate its use in more general settings. With Theorem 1 at hand, we are now ready to state our results regarding the asymptotic convergence of the per-user SINR and the per-user powers.

**Theorem 2.** Consider the setting of Theorem 1, let  $\alpha_0 := \min_{1 \leq k \leq K} \{K \ell_k p_{\max,k}\}$ , then, the following equation:

$$\tau = \frac{\alpha_0}{K} \text{Trace} \left\{ \mathbf{U} \mathbf{U}^H \left( \mathbf{U} \mathbf{U}^H \frac{\alpha_0}{(1+\tau)} + \sigma^2 \mathbf{I} \right)^{-1} \right\} \quad (15)$$

admits a unique solution  $\bar{\tau}$ . Let  $\bar{d}$  be the unique solution to the following equation:

$$d = \frac{1}{K} \text{Trace} \left\{ \mathbf{U} \mathbf{U}^H \left( \mathbf{U} \mathbf{U}^H \frac{\bar{\tau}}{d(1+\bar{\tau})} + \sigma^2 \mathbf{I} \right)^{-1} \right\}$$

Then, the following convergences hold true:

$$\tau^* - \bar{\tau} \xrightarrow[M \rightarrow \infty]{} 0 \quad (16)$$

$$\max_{1 \leq k \leq K} |d_k - \bar{d}| \xrightarrow[M \rightarrow \infty]{} 0 \quad (17)$$

$$\max_{1 \leq k \leq K} \left| p_k - \frac{\alpha_0}{\ell_k} \right| \xrightarrow[M \rightarrow \infty]{} 0. \quad (18)$$

where  $d_1, \dots, d_K$  are the unique solutions to Problem  $(\mathcal{P}_{\text{eq}})$ .

*Proof.* See Appendix C.  $\square$

1) *RIS Phase optimization using the deterministic equivalents:* Given that we have derived the asymptotic deterministic equivalent of  $\tau^*$ , we now use this to derive the optimal values of RIS phase shifts that maximize the minimum SINR. Thus, the new optimization problem can be written as follows:

$$\max_{\Phi} \bar{\tau} = \frac{\alpha_0}{K} \text{Trace} \left\{ \mathbf{U} \mathbf{U}^H \left( \frac{\alpha_0}{(1+\bar{\tau})} \mathbf{U} \mathbf{U}^H + \tilde{\sigma}^2 \mathbf{I} \right)^{-1} \right\} \quad (\mathcal{P}_3)$$

$$\text{s.t. } |\phi_n| = 1, \quad n = 1, \dots, N.$$

We use the projected gradient descent to solve the above optimization problem. We begin by evaluating the derivative of  $\bar{\tau}$  with respect to  $\phi_n$  for all  $n \in \{1, \dots, N\}$  using the implicit function theorem. Let

$$g(\bar{\tau}, \phi) = \bar{\tau} - \frac{\alpha_0}{K} \text{Trace} \{ \mathbf{U} \mathbf{U}^H \mathbf{T} \} \quad (19)$$

where  $\mathbf{T} = \left( \frac{\alpha_0}{(1+\bar{\tau})} \mathbf{U} \mathbf{U}^H + \tilde{\sigma}^2 \mathbf{I} \right)^{-1}$ , thus, we have

$$\frac{\partial \bar{\tau}}{\partial \phi_n} = - \frac{\frac{\partial g}{\partial \phi_n}}{\frac{\partial g}{\partial \bar{\tau}}} \quad (20)$$

where

$$\frac{\partial g}{\partial \bar{\tau}} = 1 - \frac{\alpha_0^2}{K(1+\bar{\tau})^2} \text{Trace} \{ \mathbf{U} \mathbf{U}^H \mathbf{T} \mathbf{U} \mathbf{U}^H \mathbf{T} \} \quad (21)$$

Evaluating  $\frac{\partial g}{\partial \phi_n}$ , we have

$$\frac{\partial g}{\partial \phi_n} = \frac{\alpha_0}{K} \left\{ \frac{\alpha_0}{1 + \bar{\tau}} \left[ \mathbf{R}_{\text{RIS}}^{\frac{1}{2}} \mathbf{H}_1^H \mathbf{T} \mathbf{R} \mathbf{H}_1 \mathbf{R}_{\text{RIS}}^{\frac{1}{2}} \Phi \mathbf{R}_{\text{users}} \right]_{n,n} - \left[ \mathbf{R}_{\text{RIS}}^{\frac{1}{2}} \mathbf{H}_1^H \mathbf{T} \mathbf{H}_1 \mathbf{R}_{\text{RIS}}^{\frac{1}{2}} \Phi \mathbf{R}_{\text{users}} \right]_{n,n} \right\} \quad (22)$$

Using (22), we implement the projected gradient descent to solve  $\mathcal{P}_3$ . Note that the solution does not depend on the instantaneous channel gains; hence, the phase optimization must only be repeated when the large-scale channel statistics vary.

2) *Power allocation using asymptotic statistics:* Note that along with the derivation for the deterministic equivalent for  $\tau^*$ , we have also established that  $\frac{\bar{\tau}}{d} = p_k \ell_k = \alpha_0$ . From this relation, we can observe that asymptotically, the power allocation for the  $k$ -th user converges to

$$\bar{p}_k = \frac{\alpha_0}{\ell_k}, \quad (23)$$

where we recall that  $\alpha_0 = \min \{ \ell_k p_{\max,k} \}$ . In the next section, we also compare the performance of this power allocation scheme with the scheme discussed in subsection III-A.

#### IV. EMF AWARE DESIGN USE CASE

This section presents one interesting application where the proposed resource allocation policy can be utilized. In problem  $\mathcal{P}_1$ , we would like to include the additional constraint that the EMF of each user is below a permissible limit. The EMF of the  $k$ -th user transmitting with a power  $p_k$  can be evaluated as  $\text{SAR}_{\text{ref},k} p_k$  where  $\text{SAR}_{\text{ref},k}$  is the SAR for user  $k$  when the transmitted power is unity. The max-min SINR optimization with constraints on the user's exposure can be expressed as follows:

$$\begin{aligned} & \max_{\{p_k\}, \phi, \beta} \quad \min_k \text{SINR}_k \\ \text{s.t.} \quad & 0 \leq \text{SAR}_{\text{ref},k} p_k \leq \text{SAR}_{\max,k} \quad \forall k \in \{1, \dots, K\} \\ & 0 \leq p_k \leq \tilde{p}_{\max}, \quad \forall k \in \{1, \dots, K\} \\ & \|\beta_k\| = 1; \quad \forall k \in \{1, \dots, K\} \\ & |\phi_n| = 1, \quad \forall n \in \{1, \dots, N\}. \end{aligned} \quad (\mathcal{P}_2)$$

Here,  $p_{\max}$  is the maximum transmit power of each user and  $\text{SAR}_{\max,k}$  is the maximum allowed exposure for user  $k$ . Note that the two constraints on the power variable can be combined and expressed as  $0 \leq p_k \leq \min \left\{ \tilde{p}_{\max}, \frac{\text{SAR}_{\max,k}}{\text{SAR}_{\text{ref},k}} \right\}$ . Let  $\min \left\{ \tilde{p}_{\max}, \frac{\text{SAR}_{\max,k}}{\text{SAR}_{\text{ref},k}} \right\} := \tilde{p}_{\max,k}$ . Then, we can notice that the problem in  $\mathcal{P}_2$  is equivalent to the one in  $\mathcal{P}_1$  for  $\tilde{p}_{\max,k} = K p_{\max,k}$ , and hence can

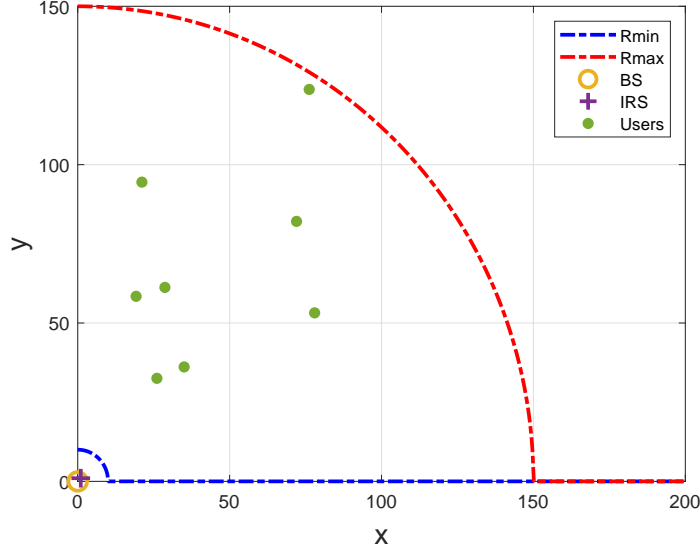


Fig. 1: Sample user, BS and IRS positions according to the simulation model used

be solved using the method proposed in the previous section. In the next section, we present simulation results for this application and hence demonstrate the performance of the proposed solution methodology.

## V. SIMULATION RESULTS

Figure 1 shows a sample realization of the simulation setup. Here we consider a simulation area similar to [22], [27], where the BS is located at the origin, and the RIS is situated at a point  $(0.5, 0.5)$  with respect to the BS. The users are uniformly spread between the area of overlap between the first quadrant and two circles of radius  $R_{\min} = 10\text{m}$  and  $R_{\max} = 70\text{m}$ , representing the exclusion zone and cell coverage, respectively.

The channel between the BS and RIS and the RIS and the  $k$ -th user are given by  $\mathbf{H}_1 = \sqrt{\frac{\text{PL}_{\text{LOS}}(d^{\text{RB}})}{N}} \left( \sqrt{\frac{\kappa}{\kappa+1}} \bar{\mathbf{H}}_1 + \sqrt{\frac{1}{\kappa+1}} \tilde{\mathbf{H}}_1 \right)$  and  $\mathbf{h}_k^u = \sqrt{\text{PL}_{\text{NLOS}}(d_k^{\text{UR}})} \tilde{h}_k^u$  respectively. Here,  $\text{PL}_{\text{LOS}}(d)$  and  $\text{PL}_{\text{NLOS}}(d)$  are the path losses experienced by the LOS and NLOS links at a distance of  $d$  from the transmitter and are modeled using the 3GPP Urban Micro (UMi) scenario from [33, Table B.1.2.1-1]. Throughout the simulations, they are chosen as  $\text{PL}_{\text{LOS}}(d) = \frac{10 \frac{G_t + G_r - 35.95}{10}}{d^{2.2}}$  and  $\text{PL}_{\text{NLOS}}(d) = \frac{10 \frac{G_t + G_r - 33.05}{10}}{d^{3.67}}$ , where  $G_t$  and  $G_r$  denote the antenna gains (in dBi) at the transmitter and receiver respectively. It is assumed that the elements of BS have 5 dBi gain while each user antenna and the RIS elements have 0 dBi gain. Here,  $\kappa$  is the Rician factor of the link between

the BS and the RIS and is chosen to be 10 throughout the simulations. The elements of the  $M \times N$  matrix  $\bar{\mathbf{H}}_1$  is given by,

$$\begin{aligned} [\bar{\mathbf{H}}_1]_{m,n} = & \exp \left[ \frac{j2\pi}{\lambda} ((m-1)d_{\text{BS}} \sin(\theta_{\text{LoS},1}(n)) \sin(\phi_{\text{LoS},1}(n)) \right. \\ & \left. + (n-1)d_{\text{RIS}} \sin(\theta_{\text{LoS},2}(m)) \sin(\phi_{\text{LoS},2}(m))) \right], \end{aligned} \quad (24)$$

where  $\theta_{\text{LoS},i}(n)$  and  $\phi_{\text{LoS},i}(n)$  for  $i \in \{1, 2\}$  and  $n \in \{1, \dots, N\}$ , are generated uniformly between 0 to  $\pi$  and 0 to  $2\pi$  respectively, [20]. Here,  $d_{\text{BS}} = 0.5\lambda$  and  $d_{\text{RIS}} = 0.5\lambda$  are the inter-antenna separation at the BS and the inter-element separation at the RIS respectively. Each of the elements of  $\tilde{\mathbf{H}}_1$  and  $\tilde{\mathbf{h}}_k^u$  are standard normal RVs. Finally,  $\mathbf{H}_k$  is defined as  $\mathbf{H}_k = [\mathbf{h}_1^u \dots \mathbf{h}_K^u]$ . Similarly, in the current set of simulations, we assume that all the users are data users and hence have  $\text{SAR}_{\text{ref},k} = 63 \times 10^{-4}$  W/Kg per unit power and  $\text{SAR}_{\text{max},k} = 0.0029$  for all  $k \in \{1, \dots, K\}$ . Similarly, the noise power in dBm is chosen as  $\sigma^2 = -174 + 10 \log_{10} B$  where the bandwidth for the data user is chosen as 100 MHz. The maximum transmit power of each user ( $p_{\text{max}}$ ) is chosen as 500 mW.

Throughout the simulations, we compare the performance of the proposed optimization scheme with the results obtained using instantaneous CSI. Here, the BF and power allocation strategy discussed in sub-section III-A are used. The RIS phase optimization is performed using the scheme discussed in [22], where a smooth approximation for the minimum is used and projected gradient descent is used to find the optimal phase shift vector. The different schemes compared in this paper are summarized in Table II.

Figure 2 and Figure 3 compares the different schemes in terms of the minimum SINR and the time taken for evaluation, respectively. We can observe that the scheme which uses the asymptotic statistics for the phase optimization alone (Scheme 2) performs close to the scheme using the instantaneous channel gains (Scheme 1). Moreover, the time taken for the alternating optimization routine using the deterministic equivalent (Scheme 2) is considerably less than the scheme using the approximation for the minimum function (Scheme 1). We can also observe that there is a severe drop in the minimum SNR when both the power allocation and phase optimization routines are performed using the deterministic equivalent (Scheme 3). Thus, we can conclude that optimal power allocation is critical for system performance. However, the small computation time for the later scheme can be utilized to generate a good initial point for performing the phase optimization using other gradient-based schemes discussed in [22], including the scheme using the approximation for the minimum.

	BF	Power Allocation	RIS Phases
Scheme 1	Instantaneous (sub-section III-A)	Instantaneous (sub-section III-A)	Instantaneous [22]
Scheme 2	Instantaneous (sub-section III-A)	Instantaneous (sub-section III-A)	Statistical (subsection III-B1)
Scheme 3	Instantaneous (sub-section III-A)	Statistical (sub-section III-B2)	Statistical (subsection III-B1)
Scheme 4	Instantaneous (sub-section III-A)	Statistical (sub-section III-B2)	$\theta_n = 0$ $\forall n \in \{1, \dots, N\}$
Scheme 5	Instantaneous (sub-section III-A)	Instantaneous (sub-section III-A)	$\theta_n = 0$ $\forall n \in \{1, \dots, N\}$
Scheme 6	Instantaneous (sub-section III-A)	Instantaneous (sub-section III-A)	$\theta_n \sim \text{Unif}[0, 2\pi]$ $\forall n \in \{1, \dots, N\}$

TABLE II: CSI assumptions for BF, power allocation and phase shift designs in different schemes compared

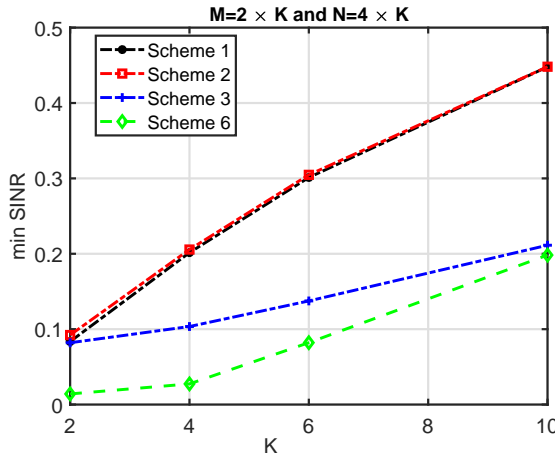


Fig. 2: Minimum SINR vs  $K$

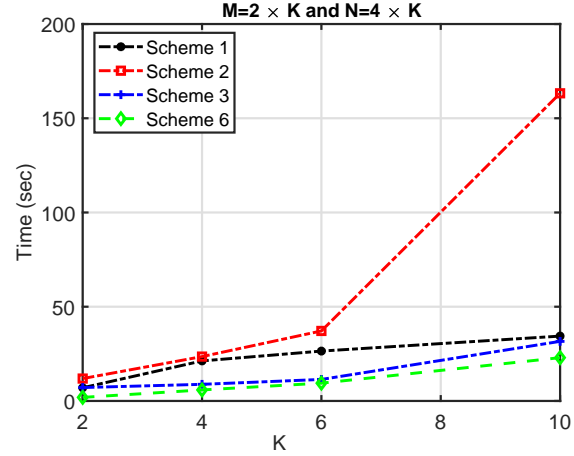


Fig. 3: Time for evaluation vs  $K$

Next, in Fig 4 we study the variation in minimum SINR with increasing values of the maximum transmit power. Note that the maximum allowable transmit power is limited by the exposure constraints, and hence beyond a specific point, increasing the transmit power will not increase the minimum SINR.

We demonstrate the significance of the optimal phase shifts at the RIS elements in Fig 5. Here, we compare the performance of Schemes 2 and 3 with the performance achieved by the same setup, except that the RIS is set to introduce no phase shift at the incoming wave. The

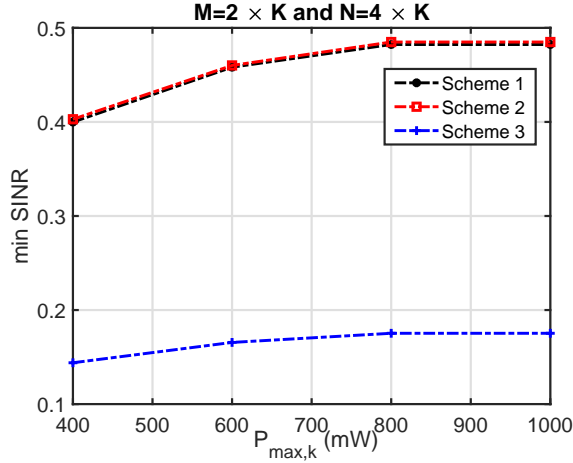
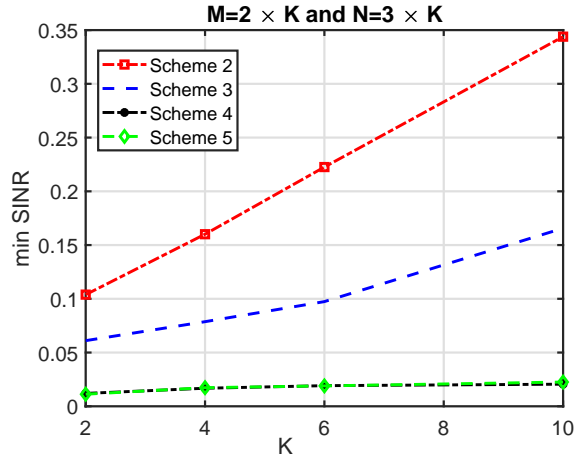
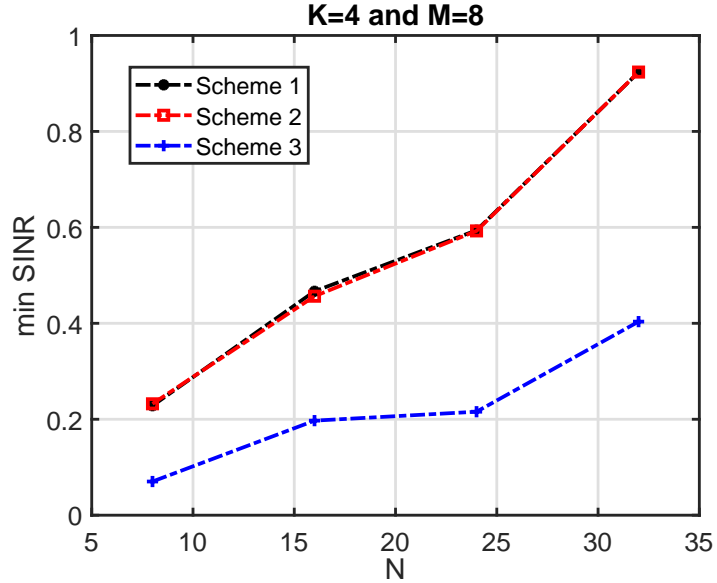
Fig. 4: Minimum SINR vs  $p_{\max}$ Fig. 5: Minimum SINR vs  $K$ Fig. 6: Minimum SINR vs  $N$ 

figure shows that the performance degrades drastically without the phase shifts introduced by the RIS. Scheme 2 was consistently demonstrating superior performance with respect to Scheme 3; however, we can see that with the change in phase shifts, Scheme 5 achieves a very low minimum SINR. Moreover, without the right choice of phase shifts, we can see that Schemes 4 and 5 demonstrate almost similar performance. This further reiterates the significance of the right choice of phase shifts at the RIS to leverage the system utility.

In Figure 6, we demonstrate the variation in minimum SINR with an increasing number of RIS elements. As expected, the minimum SINR increases with increasing  $N$ . This further suggests

that for a system with a fixed number of users and a given number of antennas at the BS, we can improve the system performance by using a RIS with more reflecting elements. Furthermore, we can see that Scheme 2 can achieve almost the same performance achieved using Scheme 1. This means, using the asymptotic statistics only, we can achieve what we were achieving using the instantaneous CSI. Scheme 2 needs much fewer computations, and feedback overhead compared to the methods using instantaneous CSI is also to be noted.

## VI. CONCLUSION

We consider the uplink communication of a RIS-assisted system and study the joint optimization of the BF vectors, power allocation, and the phase shifts at the RIS elements. A simple projected gradient descent-based optimization strategy is proposed to identify the optimal phase shift vector at the RIS elements that maximize the minimum SINR subject to constraints on the power consumed by the users. The proposed solution depends only on the asymptotic channel statistics and hence needs to be updated only when the large-scale channel statistics change. The simulations demonstrate that the minimum SINR achieved using the solution is very close to the minimum SINR achieved using the phase vector designed using the instantaneous channel statistics. Furthermore, the numerical results show that the proposed algorithms achieve more than 100% gain in terms of minimum SINR, compared to a system with random RIS phase shifts, with 40 RIS elements, 20 antennas at the BS, and 10 users.

## APPENDIX A

### SOME USEFUL RESULTS

**Lemma 1.** (*Convergence of Quadratic Forms*): Let  $\mathbf{y} \sim \mathcal{CN}(\mathbf{0}_M, \mathbf{I}_M)$ . Let  $\mathbf{A}$  be an  $M \times M$  matrix independent of  $\mathbf{y}$ , which has a bounded spectral norm. Then  $\frac{1}{M}\mathbf{y}^H \mathbf{A} \mathbf{y} - \frac{1}{M} \text{tr}(\mathbf{A}) \xrightarrow[n \rightarrow \infty]{a.s.} 0$ .

**Lemma 2.** Consider the  $M \times M$  matrix:

$$\mathbf{B} = \frac{1}{K} \mathbf{U} \mathbf{X} \mathbf{X}^H \mathbf{U}^H$$

with the following Assumptions:

- 1)  $\mathbf{X} \in \mathbb{C}^{N \times K}$  is such that  $[\mathbf{X}]_{ij}$  are identically distributed and independent and  $\text{var}([\mathbf{X}]_{ij}) = 1$  and finite fourth order moments.
- 2)  $\mathbf{R} = \mathbf{U} \mathbf{U}^H$  with  $\mathbf{U} \in \mathbb{C}^{M \times N}$  has uniformly bounded spectral norm over  $M$  and  $N$ .

3) Denoting  $c_1 = \frac{K}{M}$  and  $c_0 = \frac{N}{K}$ , then

$$0 < \liminf c_1 < \infty \text{ and } 0 < c_0 < \infty$$

Then, as all  $M, K$  and  $N$  grow large with ratios  $c_1$  and  $c_0$ , for  $z \in \mathbb{C} \setminus \mathbb{R}^+$ , and for all non-negative hermitian matrices  $\mathbf{C} \in \mathbb{C}^{N \times N}$  with uniformly bounded spectral norm:

$$\frac{1}{K} \text{Trace} \left\{ \mathbf{C} (\mathbf{B} - z\mathbf{I})^{-1} \right\} - \frac{1}{K} \text{Trace} \left\{ \mathbf{C} \left( -z\mathbf{I} + \frac{\mathbf{R}}{1+e(z)} \right)^{-1} \right\}$$

converges almost surely to zero where  $e(z)$  form the unique solution of

$$e(z) = \frac{1}{K} \text{Trace} \left\{ \mathbf{R} \left( -z\mathbf{I} + \frac{\mathbf{R}}{1+e(z)} \right)^{-1} \right\}$$

## APPENDIX B

### PROOF OF THEOREM 1

We start by proving the following equation:

$$d = \frac{1}{K} \text{Trace} \left\{ \mathbf{U} \mathbf{U}^H \left( \mathbf{U} \mathbf{U}^H \frac{\tau}{d(1+\tau)} + \sigma^2 \mathbf{I} \right)^{-1} \right\} \quad (25)$$

admits a unique solution  $\bar{d}(\tau)$ . Dividing both sides in (25) by  $\bar{d}(\tau)$ , we obtain:

$$1 = \frac{1}{K} \text{Trace} \left\{ \mathbf{U} \mathbf{U}^H \left( \mathbf{U} \mathbf{U}^H \frac{\tau}{(1+\tau)} + \sigma^2 \bar{d}(\tau) \mathbf{I} \right)^{-1} \right\} \quad (26)$$

Function  $h_\tau : d \mapsto \frac{1}{K} \text{Trace} \left\{ \mathbf{U} \mathbf{U}^H \left( \mathbf{U} \mathbf{U}^H \frac{\tau}{(1+\tau)} + \sigma^2 d \mathbf{I} \right)^{-1} \right\}$  is decreasing. Since  $K/M < 1$ ,  $\lim_{d \rightarrow 0} h_\tau(d) > 1$ . As  $\lim_{d \rightarrow \infty} h_\tau(d) = 0$ , there exists a unique  $\bar{d}(\tau)$  satisfying  $h_\tau(\bar{d}(\tau)) = 1$ , which shows existence and uniqueness of the solution to (25). On the other hand, since  $\lim_{d \rightarrow \infty} \sup_{\tau \geq 0} h_\tau(d) = 0$ , there exists  $C$  such that  $\sup_{\tau \geq 0} \bar{d}(\tau) < C$ . Now, since  $h(0) \geq \frac{1+\tau}{\tau} \liminf \frac{M}{K} > 1$ , we also have  $\inf_{\tau \geq 0} \bar{d}(\tau) > 0$ .

The next step is now to show that:

$$\sup_{\tau \in \mathcal{I}} \max_{1 \leq k \leq K} \left| \frac{d_k(\tau)}{\bar{d}(\tau)} - 1 \right| \xrightarrow{M \rightarrow \infty} 0$$

where  $d_1(\tau), \dots, d_K(\tau)$  are the unique solutions to the system of equations in (11). Letting  $e_k(\tau) := \frac{d_k(\tau)}{\bar{d}(\tau)}$ , this amounts to showing that for all  $\ell > 0$ , we have for sufficiently large dimensions:

$$\forall \tau \in \mathcal{I}, \quad k = 1, \dots, K, \quad -\ell \leq e_k(\tau) - 1 \leq \ell. \quad (27)$$

Assume without loss of generality that  $e_1(\tau) < e_2(\tau) < \dots < e_K(\tau)$ . Proving (27) is thus equivalent to showing the following inequalities:

$$\forall \tau \in \mathcal{I}, \quad e_K(\tau) \leq 1 + \ell \quad (28)$$

$$\forall \tau \in \mathcal{I}, \quad e_1(\tau) \geq 1 - \ell \quad (29)$$

Proof of (28). Starting off from the expression of  $d_k(\tau)$ , we may express  $e_k(\tau)$  as:

$$e_k(\tau) = \frac{1}{K\bar{d}(\tau)} \tilde{\mathbf{h}}_{2,k}^H \mathbf{U}^H \left( \sum_{i \neq k} \frac{\tau}{Kd_i(\tau)} \mathbf{U} \tilde{\mathbf{h}}_{2,i} \tilde{\mathbf{h}}_{2,i}^H \mathbf{U}^H + \sigma^2 \mathbf{I} \right)^{-1} \mathbf{U} \tilde{\mathbf{h}}_{2,k}, \quad (30)$$

$$= \frac{1}{K} \tilde{\mathbf{h}}_{2,k}^H \mathbf{U}^H \left( \sum_{i \neq k} \frac{\tau}{Ke_i(\tau)} \mathbf{U} \tilde{\mathbf{h}}_{2,i} \tilde{\mathbf{h}}_{2,i}^H \mathbf{U}^H + \sigma^2 \bar{d}(\tau) \mathbf{I} \right)^{-1} \mathbf{U} \tilde{\mathbf{h}}_{2,k} \quad (31)$$

Evaluating (31) for  $k = K$ , we obtain:

$$e_K(\tau) = \frac{1}{K} \tilde{\mathbf{h}}_{2,K}^H \mathbf{U}^H \left( \sum_{i \neq K} \frac{\tau}{Ke_i(\tau)} \mathbf{U} \tilde{\mathbf{h}}_{2,i} \tilde{\mathbf{h}}_{2,i}^H \mathbf{U}^H + \sigma^2 \bar{d}(\tau) \mathbf{I} \right)^{-1} \mathbf{U} \tilde{\mathbf{h}}_{2,K}$$

Since  $e_K(\tau) \geq e_i(\tau)$  for all  $i \neq K$ , we have:

$$e_K(\tau) \leq \frac{1}{K} \tilde{\mathbf{h}}_{2,K}^H \mathbf{U}^H \left( \sum_{i \neq K} \frac{\tau}{Ke_K(\tau)} \mathbf{U} \tilde{\mathbf{h}}_{2,i} \tilde{\mathbf{h}}_{2,i}^H \mathbf{U}^H + \sigma^2 \bar{d}(\tau) \mathbf{I} \right)^{-1} \mathbf{U} \tilde{\mathbf{h}}_{2,K}$$

or equivalently:

$$1 \leq \frac{1}{K} \tilde{\mathbf{h}}_{2,K}^H \mathbf{U}^H \left( \sum_{i \neq K} \frac{\tau}{K} \mathbf{U} \tilde{\mathbf{h}}_{2,i} \tilde{\mathbf{h}}_{2,i}^H \mathbf{U}^H + \sigma^2 \bar{d}(\tau) e_K(\tau) \mathbf{I} \right)^{-1} \mathbf{U} \tilde{\mathbf{h}}_{2,K} \quad (32)$$

Recall that our objective is to prove that for sufficiently large dimensions:

$$\sup_{\tau \in \mathcal{I}} e_K(\tau) \leq 1 + \ell$$

or equivalently:

$$\limsup_{N,M,K} \sup_{\tau \in \mathcal{I}} e_K(\tau) \leq 1 + \ell$$

For that, we proceed by contradiction and assume that:

$$\limsup_{N,M,K} \sup_{\tau \in \mathcal{I}} e_K(\tau) \geq 1 + \ell \quad (33)$$

Hence, in view of (32), for  $N, K$  and  $M$  sufficiently large, there exists  $\tilde{\tau} \in \mathcal{I}$  such that:

$$1 \leq \frac{1}{K} \tilde{\mathbf{h}}_{2,K}^H \mathbf{U}^H \left( \sum_{i \neq K} \frac{\tilde{\tau}}{K} \mathbf{U} \tilde{\mathbf{h}}_{2,i} \tilde{\mathbf{h}}_{2,i}^H \mathbf{U}^H + \sigma^2 \bar{d}(\tilde{\tau})(1 + \ell) \mathbf{I} \right)^{-1} \mathbf{U} \tilde{\mathbf{h}}_{2,K}$$

To continue, we apply Lemma 1 and Lemma 2 to study the asymptotic limit of the right-hand side term of the above inequality. Indeed, the following convergence holds point-wise in  $\tau$ :

$$\frac{1}{K} \tilde{\mathbf{h}}_{2,K}^H \mathbf{U}^H \left( \sum_{i \neq K} \frac{\tau}{K} \mathbf{U} \tilde{\mathbf{h}}_{2,i} \tilde{\mathbf{h}}_{2,i}^H \mathbf{U}^H + \sigma^2 \bar{d}(\tau)(1 + \ell) \mathbf{I} \right)^{-1} \mathbf{U} \tilde{\mathbf{h}}_{2,K} - \mu \xrightarrow[M \rightarrow \infty]{\text{a.s.}} 0 \quad (34)$$

where  $\mu(\tau)$  is the unique solution to the following equation:

$$\mu(\tau) = \frac{1}{K} \text{Trace} \left\{ \mathbf{U} \mathbf{U}^H \left( \sigma^2 \bar{d}(\tau)(1 + \ell) \mathbf{I} + \frac{\tau \mathbf{U} \mathbf{U}^H}{1 + \mu(\tau) \tau} \right)^{-1} \right\}$$

Since function  $(\tau, d) \mapsto \frac{1}{K} \tilde{\mathbf{h}}_{2,K}^H \mathbf{U}^H \left( \sum_{i \neq K} \frac{\tau}{K} \mathbf{U} \tilde{\mathbf{h}}_{2,i} \tilde{\mathbf{h}}_{2,i}^H \mathbf{U}^H + \sigma^2 \bar{d}(\tau)(1 + \ell) \mathbf{I} \right)^{-1} \mathbf{U} \tilde{\mathbf{h}}_{2,K}$  is Lipschitz on any compact set in  $(0, \infty) \times (0, \infty)$ , by Arzela-Ascoli theorem, the convergence in (34) hold uniformly in  $\tau$  and  $\bar{d}(\tau)$  belonging to compact sets in  $(0, \infty) \times (0, \infty)$ . As we proved earlier that  $\bar{d}(\tau)$  lies in a compact set when  $\tau \in \mathcal{I}$ , we obtain:

$$\sup_{\tau \in \mathcal{I}} \left| \frac{1}{K} \tilde{\mathbf{h}}_{2,K}^H \mathbf{U}^H \left( \sum_{i \neq K} \frac{\tau}{K} \mathbf{U} \tilde{\mathbf{h}}_{2,i} \tilde{\mathbf{h}}_{2,i}^H \mathbf{U}^H + \sigma^2 \bar{d}(\tau)(1 + \ell) \mathbf{I} \right)^{-1} \mathbf{U} \tilde{\mathbf{h}}_{2,K} - \mu \right| \xrightarrow[M \rightarrow \infty]{} 0$$

In other words, for any  $\epsilon$  sufficiently small and positive, and sufficiently large  $N, K$  and  $M$ :

$$\forall \tau \in \mathcal{I}, \quad \frac{1}{K} \tilde{\mathbf{h}}_{2,K}^H \mathbf{U}^H \left( \sum_{i \neq K} \frac{\tau}{K} \mathbf{U} \tilde{\mathbf{h}}_{2,i} \tilde{\mathbf{h}}_{2,i}^H \mathbf{U}^H + \sigma^2 \bar{d}(\tau)(1 + \ell) \mathbf{I} \right)^{-1} \mathbf{U} \tilde{\mathbf{h}}_{2,K} \leq \mu(\tau) + \epsilon$$

Particularly, for  $\tau = \tilde{\tau}$ , we obtain:

$$\frac{1}{K} \tilde{\mathbf{h}}_{2,K}^H \mathbf{U}^H \left( \sum_{i \neq K} \frac{\tilde{\tau}}{K} \mathbf{U} \tilde{\mathbf{h}}_{2,i} \tilde{\mathbf{h}}_{2,i}^H \mathbf{U}^H + \sigma^2 \bar{d}(\tilde{\tau})(1 + \ell) \mathbf{I} \right)^{-1} \mathbf{U} \tilde{\mathbf{h}}_{2,K} \leq \mu(\tilde{\tau}) + \epsilon \quad (35)$$

To show contradiction to (33), it suffices to prove that for all  $\tau \in \mathcal{I}$ ,  $\mu(\tau) < 1$ . Indeed, if  $\forall \tau \in \mathcal{I}$ ,  $\mu(\tau) < 1$ , then by choosing  $\epsilon < \ell$ , the inequality in (35) becomes in contradiction to (33). Recalling that  $\mu(\tau)$  is the unique solution to the following equation:

$$\mu(\tau) = \frac{1}{K} \text{Trace} \left\{ \mathbf{U} \mathbf{U}^H \left( \sigma^2 \bar{d}(\tau)(1 + \ell) \mathbf{I} + \frac{\tau \mathbf{U} \mathbf{U}^H}{1 + \mu(\tau) \tau} \right)^{-1} \right\}$$

Dividing both sides by  $\mu(\tau)$ , we obtain:

$$1 = \frac{1}{K} \text{Trace} \left\{ \mathbf{U} \mathbf{U}^H \left( \sigma^2 \mu(\tau) \bar{d}(\tau)(1 + \ell) \mathbf{I} + \frac{\mu(\tau) \tau \mathbf{U} \mathbf{U}^H}{1 + \mu(\tau) \tau} \right)^{-1} \right\} \quad (36)$$

Let  $g : \mu \mapsto \frac{1}{K} \text{Trace} \left\{ \mathbf{U} \mathbf{U}^H \left( \sigma^2 \mu \bar{d}(\tau) (1 + \ell) \mathbf{I} + \frac{\mu \tau \mathbf{U} \mathbf{U}^H}{1 + \mu \tau} \right)^{-1} \right\}$ . Then,  $g$  is a decreasing function of  $\mu$ . Moreover,

$$g(1) = \frac{1}{K} \text{Trace} \left\{ \mathbf{U} \mathbf{U}^H \left( \sigma^2 \bar{d}(\tau) (1 + \ell) \mathbf{I} + \frac{\tau \mathbf{U} \mathbf{U}^H}{1 + \tau} \right)^{-1} \right\} \quad (37)$$

$$< \frac{1}{K} \text{Trace} \left\{ \mathbf{U} \mathbf{U}^H \left( \sigma^2 \bar{d}(\tau) \mathbf{I} + \frac{\tau \mathbf{U} \mathbf{U}^H}{1 + \tau} \right)^{-1} \right\} = 1 \quad (38)$$

where in the last equality, we used (26). If  $\mu(\tau) \geq 1$ , then since  $g$  is decreasing  $g(\mu(\tau)) \leq g(1) < 1$ , creating a contradiction with (36). Hence,  $\mu(\tau) < 1$ . This completes the proof of (28). The proof of (29) follows the same lines and is thus omitted.

## APPENDIX C PROOF OF THEOREM 2

**Strategy of the proof.** We organize the proof of Theorem 2 in two parts. In the first part, denoting by  $\alpha_k = K \ell_k p_{\max, k}$ ,  $k \in \{1, \dots, K\}$ , we prove that the optimal cost of the following problem:

$$\begin{aligned} \tau^* &= \max_{d_k, \tau} \quad \tau \\ \text{s.t.} \quad d_k(\tau) &= h_k(d_1, \dots, d_K; \tau), \quad k = 1, \dots, K \\ \frac{\tau}{d_k(\tau)} &\leq \alpha_k, \quad k = 1, \dots, K. \end{aligned} \quad (\hat{\mathcal{P}})$$

is asymptotically equivalent to the optimal cost of the following deterministic problem:

$$\begin{aligned} \tilde{\tau} &= \max_{d, \tau} \quad \tau \\ \text{s.t.} \quad d &= \frac{1}{K} \text{Trace} \left\{ \mathbf{U} \mathbf{U}^H \left( \mathbf{U} \mathbf{U}^H \frac{\tau}{d(1 + \tau)} + \sigma^2 \mathbf{I} \right)^{-1} \right\} \\ \frac{\tau}{d} &\leq \alpha_k, \quad k = 1, \dots, K \end{aligned} \quad (\mathcal{P}_{\text{asym}})$$

in the sense that  $\tau^* - \tilde{\tau} \xrightarrow[M \rightarrow \infty]{} 0$ . In the second part, we show that  $\tilde{\tau}$  is equal to  $\bar{\tau}$ , the unique solution to (15). Finally, by combining the findings of Theorem 1 along with those of both parts, we deduce the convergence results of Theorem 2.

**First part.** Let  $(\tilde{\tau}, \tilde{d})$  be the solution to  $(\mathcal{P}_{\text{asym}})$ . The uniqueness of this solution is a straightforward consequence of the second part of the proof and thus will be admitted here. Our goal in this section is to show that  $\tau^* - \tilde{\tau} \xrightarrow[M \rightarrow \infty]{} 0$ .

Before delving into the proof, we need first to check that the solution  $\tau^*$  to  $\hat{\mathcal{P}}$  lies almost surely

in a compact set in  $(0, \infty)$  to enable the use of the results of Theorem 1. For that, we use the fact that for any feasible  $\tau, d_k$  such  $\frac{\tau}{d_k} \leq \alpha_k$ , we have:

$$\frac{1}{K} \tilde{\mathbf{g}}_k^H \left( \sum_{i \neq k} \alpha_i \tilde{\mathbf{g}}_i \tilde{\mathbf{g}}_i^H + \sigma^2 \mathbf{I} \right)^{-1} \tilde{\mathbf{g}}_k \leq d_k = h_k(d_1, \dots, d_K; \tau) \leq \frac{1}{K \sigma^2} \tilde{\mathbf{g}}_k^H \mathbf{g}_k$$

From standard results of random matrix theory, under the regime growth of Assumption 1 and Assumption 2, there exists strictly positive constants  $C_1$  and  $C_2$  such that almost surely,

$$\forall k = 1, \dots, K, \quad \frac{1}{K} \tilde{\mathbf{g}}_k^H \left( \sum_{i \neq k} \alpha_i \tilde{\mathbf{g}}_i \tilde{\mathbf{g}}_i^H + \sigma^2 \mathbf{I} \right)^{-1} \tilde{\mathbf{g}}_k \geq C_1 \quad \text{and} \quad \frac{1}{K \sigma^2} \tilde{\mathbf{g}}_k^H \tilde{\mathbf{g}}_k \leq C_2$$

Hence, for any feasible  $\tau$ , we have:

$$\tau \leq C_2 \alpha_0 \quad \text{and} \quad \tau \geq \alpha_0 C_1$$

which proves that  $\tau$  lies almost surely in a compact set of  $(0, \infty)$ . Let  $\mathcal{I}$  be a compact interval in  $(0, \infty)$  containing  $(C_1 \alpha_0, C_2 \alpha_0)$ . We may thus exploit Theorem 1 to show that:

$$\sup_{\tau \in \mathcal{I}} \max_{1 \leq k \leq K} \left| \frac{\tau}{d_k(\tau)} - \frac{\tau}{\bar{d}(\tau)} \right| \xrightarrow{M \rightarrow \infty} 0$$

Hence, for any  $\delta > 0$ , there exists  $N_0, M_0$  and  $K_0$  such that for all  $N \geq N_0, M \geq M_0$  and  $K \geq K_0$ , we have:

$$\forall \tau \in \mathcal{I} \quad \forall k = 1, \dots, K \quad \frac{\tau}{\bar{d}(\tau)} - \delta \leq \frac{\tau}{d_k(\tau)} \leq \frac{\tau}{\bar{d}(\tau)} + \delta \quad (39)$$

Now, consider the following perturbed asymptotically equivalent problems:

$$\begin{aligned} \tilde{\tau}_{\delta^+} &= \max_{d, \tau} \quad \tau \\ \text{s.t.} \quad d &= \frac{1}{K} \text{Trace} \left\{ \mathbf{U} \mathbf{U}^H \left( \mathbf{U} \mathbf{U}^H \frac{\tau}{d(1+\tau)} + \sigma^2 \mathbf{I} \right)^{-1} \right\} \\ \frac{\tau}{d} &\leq \alpha_k + \delta, \quad k = 1, \dots, K \end{aligned} \quad (\mathcal{P}_{\text{asym}}^+)$$

and

$$\begin{aligned} \tilde{\tau}_{\delta^-} &= \max_{d, \tau} \quad \tau \\ \text{s.t.} \quad d &= \frac{1}{K} \text{Trace} \left\{ \mathbf{U} \mathbf{U}^H \left( \mathbf{U} \mathbf{U}^H \frac{\tau}{d(1+\tau)} + \sigma^2 \mathbf{I} \right)^{-1} \right\} \\ \frac{\tau}{d} &\leq \alpha_k - \delta, \quad k = 1, \dots, K \end{aligned} \quad (\mathcal{P}_{\text{asym}}^-)$$

The main idea is to show that almost surely, for sufficiently large dimensions:

$$\tilde{\tau}_{\delta^-} \leq \tau^* \leq \tilde{\tau}_{\delta^+} \quad (40)$$

Then, based on Lemma 9 in [34], we have

$$\lim_{\delta \rightarrow 0} \tilde{\tau}_{\delta^-} = \tilde{\tau}$$

and

$$\lim_{\delta \rightarrow 0} \tilde{\tau}_{\delta^+} = \tilde{\tau}$$

Hence, for any  $\epsilon > 0$ , we may choose  $\delta$  sufficiently small such that:

$$\tilde{\tau} \geq \tilde{\tau}_{\delta^+} - \epsilon \quad \text{and} \quad \tilde{\tau} \leq \tilde{\tau}_{\delta^-} + \epsilon \quad (41)$$

By combining this with (40), we thus obtain

$$\tilde{\tau} - \epsilon \leq \tau^* \leq \tilde{\tau} + \epsilon$$

which shows the desired. We will thus focus in the sequel on establishing both inequalities in (40).

**Proof of  $\tau^* \leq \tilde{\tau}_{\delta^+}$ .** Let  $\tau$  be feasible for Problem  $\hat{\mathcal{P}}$ . To prove the desired, it suffices to show that  $\tau$  is feasible for Problem  $\mathcal{P}_{\text{asym}}^+$ . Indeed, it follows from (39) that:

$$\frac{\tau}{\bar{d}(\tau)} - \delta \leq \frac{\tau}{d_k(\tau)} \leq \alpha_k$$

and hence

$$\frac{\tau}{\bar{d}(\tau)} \leq \alpha_k + \delta$$

This proves that  $\tau$  is feasible for  $\mathcal{P}_{\text{asym}}^+$  and thus  $\tau^* \leq \tilde{\tau}_{\delta^+}$ .

**Proof of  $\tau^* \geq \tilde{\tau}_{\delta^-}$ .** Let  $\tau$  be feasible for  $\mathcal{P}_{\text{asym}}^-$ . Then,  $\frac{\tau}{\bar{d}(\tau)} \leq \alpha_k - \delta$ . Using (39), we thus get:

$$\frac{\tau}{\bar{d}_k(\tau)} - \delta \leq \alpha_k - \delta$$

or equivalently

$$\frac{\tau}{d_k(\tau)} \leq \alpha_k$$

Hence  $\tau$  is feasible for  $\hat{\mathcal{P}}$  and thus  $\tau^* \geq \tilde{\tau}_{\delta^-}$

**Second part.** First, we check that (15) admits a unique solution. Indeed, by dividing both sides of (15), we obtain:

$$1 = \frac{\alpha_0}{K} \text{Trace} \left\{ \mathbf{U} \mathbf{U}^H \left( \frac{\mathbf{U} \mathbf{U}^H \alpha_0 \tau}{1 + \tau} + \sigma^2 \tau \mathbf{I} \right)^{-1} \right\} \quad (42)$$

The right-hand side of the above equality is a decreasing function of  $\tau$  tending to 0 as  $\tau \rightarrow \infty$  and to  $\infty$  as  $\tau$  goes to zero. Hence, there exists a unique  $\bar{\tau}$  satisfying (42). Let  $\bar{d} = \frac{\bar{\tau}}{\alpha_0}$  where

we recall that  $\alpha_0 = \min_{1 \leq k \leq K} \alpha_k$ . Our aim is to show that  $\tilde{\tau} = \bar{\tau}$  and  $\bar{d} = \check{d}$ . For that, it suffices to show that  $\frac{\tilde{\tau}}{\check{d}} = \alpha_0$ . Indeed, if this is true, then starting from

$$\check{d} = \frac{1}{K} \text{Trace} \left\{ \mathbf{U} \mathbf{U}^H \left( \mathbf{U} \mathbf{U}^H \frac{\tilde{\tau}}{\check{d}(1 + \tilde{\tau})} + \sigma^2 \mathbf{I} \right)^{-1} \right\}$$

we thus obtain:

$$\frac{\check{d}}{\tilde{\tau}} = \frac{1}{K} \text{Trace} \left\{ \mathbf{U} \mathbf{U}^H \left( \mathbf{U} \mathbf{U}^H \frac{\tilde{\tau}^2}{\check{d}(1 + \tilde{\tau})} + \tilde{\tau} \sigma^2 \mathbf{I} \right)^{-1} \right\}$$

Replacing  $\frac{\tilde{\tau}}{\check{d}}$  by  $\alpha_0$ , we thus obtain:

$$1 = \frac{\alpha_0}{K} \text{Trace} \left\{ \mathbf{U} \mathbf{U}^H \left( \mathbf{U} \mathbf{U}^H \alpha_0 \frac{\tilde{\tau}}{1 + \tilde{\tau}} + \tilde{\tau} \sigma^2 \mathbf{I} \right)^{-1} \right\}$$

or equivalently

$$\tilde{\tau} = \frac{\alpha_0}{K} \text{Trace} \left\{ \mathbf{U} \mathbf{U}^H \left( \mathbf{U} \mathbf{U}^H \alpha_0 \frac{1}{1 + \tilde{\tau}} + \sigma^2 \mathbf{I} \right)^{-1} \right\}$$

Since  $\bar{\tau}$  is the unique solution to the above equation, we thus have  $\tilde{\tau} = \bar{\tau}$ , and  $\bar{d} = \check{d}$ . In the sequel, we will thus focus on showing that  $\frac{\tilde{\tau}}{\check{d}} = \alpha_0$ . We will thus proceed by contradiction and assume that  $\frac{\tilde{\tau}}{\check{d}} < \alpha_0$ . Then, starting from:

$$\check{d} = \frac{1}{K} \text{Trace} \left\{ \mathbf{U} \mathbf{U}^H \left( \frac{\tilde{\tau}}{\check{d}(1 + \tilde{\tau})} \mathbf{U} \mathbf{U}^H + \sigma^2 \mathbf{I} \right)^{-1} \right\}$$

we have:

$$\check{d} > \frac{1}{K} \text{Trace} \left\{ \mathbf{U} \mathbf{U}^H \left( \frac{\alpha_0}{(1 + \tilde{\tau})} \mathbf{U} \mathbf{U}^H + \sigma^2 \mathbf{I} \right)^{-1} \right\} \quad (43)$$

(44)

Next, we use the fact that  $\tilde{\tau} \geq \bar{\tau}$  to obtain:

$$\check{d} > \frac{1}{K} \text{Trace} \left\{ \mathbf{U} \mathbf{U}^H \left( \frac{\alpha_0}{1 + \bar{\tau}} \mathbf{U} \mathbf{U}^H + \sigma^2 \mathbf{I} \right)^{-1} \right\} \quad (45)$$

$$= \frac{1}{K} \text{Trace} \left\{ \mathbf{U} \mathbf{U}^H \left( \frac{\bar{\tau}}{(1 + \bar{\tau}) \bar{d}} \mathbf{U} \mathbf{U}^H + \sigma^2 \mathbf{I} \right)^{-1} \right\} \quad (46)$$

or equivalently  $\check{d} > \bar{d}$ . To continue, we start from

$$\check{d} = \frac{1}{K} \text{Trace} \left\{ \mathbf{U} \mathbf{U}^H \left( \mathbf{U} \mathbf{U}^H \frac{\tilde{\tau}}{\check{d}(1 + \tilde{\tau})} + \sigma^2 \mathbf{I} \right)^{-1} \right\}$$

and use the fact that  $\tilde{\tau} \geq \bar{\tau}$  to obtain:

$$\check{d} \leq \frac{1}{K} \text{Trace} \left\{ \mathbf{U} \mathbf{U}^H \left( \mathbf{U} \mathbf{U}^H \frac{\bar{\tau}}{\check{d}(1+\bar{\tau})} + \sigma^2 \mathbf{I} \right)^{-1} \right\}$$

or equivalently:

$$\check{d} \leq \frac{\bar{d}}{K} \text{Trace} \left\{ \mathbf{U} \mathbf{U}^H \left( \mathbf{U} \mathbf{U}^H \frac{\bar{\tau}}{1+\bar{\tau}} + \sigma^2 \bar{d} \mathbf{I} \right)^{-1} \right\}$$

Now, since  $\check{d} > \bar{d}$ , we obtain:

$$\check{d} < \frac{\bar{d}}{K} \text{Trace} \left\{ \mathbf{U} \mathbf{U}^H \left( \mathbf{U} \mathbf{U}^H \frac{\bar{\tau}}{1+\bar{\tau}} + \sigma^2 \check{d} \mathbf{I} \right)^{-1} \right\} \quad (47)$$

$$\leq \frac{\bar{d}}{K} \text{Trace} \left\{ \mathbf{U} \mathbf{U}^H \left( \mathbf{U} \mathbf{U}^H \frac{\bar{\tau}}{1+\bar{\tau}} + \sigma^2 \bar{d} \mathbf{I} \right)^{-1} \right\} \quad (48)$$

or equivalently  $\check{d} < \bar{d}$ , which is in contradiction with the previously obtained inequality  $\check{d} > \bar{d}$ .

## REFERENCES

- [1] E. Basar, M. Di Renzo, J. De Rosny, M. Debbah, M.-S. Alouini, and R. Zhang, “Wireless communications through reconfigurable intelligent surfaces,” *IEEE access*, vol. 7, pp. 116 753–116 773, 2019.
- [2] Ö. Özdogan, E. Björnson, and E. G. Larsson, “Intelligent reflecting surfaces: Physics, propagation, and pathloss modeling,” *IEEE Wireless Communications Letters*, vol. 9, no. 5, pp. 581–585, 2019.
- [3] M. Di Renzo, A. Zappone, M. Debbah, M.-S. Alouini, C. Yuen, J. De Rosny, and S. Tretyakov, “Smart radio environments empowered by reconfigurable intelligent surfaces: How it works, state of research, and the road ahead,” *IEEE Journal on Selected Areas in Communications*, vol. 38, no. 11, pp. 2450–2525, 2020.
- [4] C. Liaskos, S. Nie, A. Tsoliariidou, A. Pitsillides, S. Ioannidis, and I. Akyildiz, “A new wireless communication paradigm through software-controlled metasurfaces,” *IEEE Communications Magazine*, vol. 56, no. 9, pp. 162–169, 2018.
- [5] C. Pan, H. Ren, K. Wang, W. Xu, M. Elkashlan, A. Nallanathan, and L. Hanzo, “Multicell MIMO communications relying on intelligent reflecting surfaces,” *IEEE Transactions on Wireless Communications*, vol. 19, no. 8, pp. 5218–5233, 2020.
- [6] N. S. Perović, M. Di Renzo, and M. F. Flanagan, “Channel capacity optimization using reconfigurable intelligent surfaces in indoor mmWave environments,” in *ICC 2020-2020 IEEE International Conference on Communications (ICC)*. IEEE, 2020, pp. 1–7.
- [7] X. Yu, D. Xu, and R. Schober, “Enabling secure wireless communications via intelligent reflecting surfaces,” in *2019 IEEE Global Communications Conference (GLOBECOM)*. IEEE, 2019, pp. 1–6.
- [8] S. Gopi, S. Kalyani, and L. Hanzo, “Intelligent reflecting surface assisted beam index-modulation for millimeter wave communication,” *IEEE Transactions on Wireless Communications*, vol. 20, no. 2, pp. 983–996, 2020.
- [9] H. Guo, Y.-C. Liang, J. Chen, and E. G. Larsson, “Weighted sum-rate maximization for reconfigurable intelligent surface aided wireless networks,” *IEEE Transactions on Wireless Communications*, vol. 19, no. 5, pp. 3064–3076, 2020.
- [10] X. Yu, D. Xu, and R. Schober, “MISO wireless communication systems via intelligent reflecting surfaces,” in *2019 IEEE/CIC International Conference on Communications in China (ICCC)*. IEEE, 2019, pp. 735–740.
- [11] K. Feng, Q. Wang, X. Li, and C.-K. Wen, “Deep reinforcement learning based intelligent reflecting surface optimization for MISO communication systems,” *IEEE Wireless Communications Letters*, vol. 9, no. 5, pp. 745–749, 2020.

- [12] H. Alwazani, A. Kammoun, A. Chaaban, M. Debbah, M.-S. Alouini *et al.*, “Intelligent reflecting surface-assisted multi-user MISO communication: Channel estimation and beamforming design,” *IEEE Open Journal of the Communications Society*, vol. 1, pp. 661–680, 2020.
- [13] S. Abeywickrama, R. Zhang, Q. Wu, and C. Yuen, “Intelligent reflecting surface: Practical phase shift model and beamforming optimization,” *IEEE Transactions on Communications*, vol. 68, no. 9, pp. 5849–5863, 2020.
- [14] S. Luo, P. Yang, Y. Che, K. Yang, K. Wu, K. C. Teh, and S. Li, “Spatial modulation for RIS-assisted uplink communication: Joint power allocation and passive beamforming design,” *IEEE Transactions on Communications*, vol. 69, no. 10, pp. 7017–7031, 2021.
- [15] K. Zhi, C. Pan, H. Ren, and K. Wang, “Statistical CSI-based design for reconfigurable intelligent surface-aided massive MIMO systems with direct links,” *IEEE Wireless Communications Letters*, vol. 10, no. 5, pp. 1128–1132, 2021.
- [16] J. Wang, H. Wang, Y. Han, S. Jin, and X. Li, “Joint transmit beamforming and phase shift design for reconfigurable intelligent surface assisted MIMO systems,” *IEEE Transactions on Cognitive Communications and Networking*, vol. 7, no. 2, pp. 354–368, 2021.
- [17] L. You, J. Xiong, Y. Huang, D. W. K. Ng, C. Pan, W. Wang, and X. Gao, “Reconfigurable intelligent surfaces-assisted multiuser MIMO uplink transmission with partial CSI,” *IEEE Transactions on Wireless Communications*, vol. 20, no. 9, pp. 5613–5627, 2021.
- [18] Z. Shi, H. Wang, Y. Fu, G. Yang, S. Ma, and F. Gao, “Outage Analysis of Reconfigurable Intelligent Surface Aided MIMO Communications With Statistical CSI,” *IEEE Transactions on Wireless Communications*, 2021.
- [19] M. Charishma, A. Subhash, S. Shekhar, and S. Kalyani, “Outage Probability Expressions for an IRS-Assisted System with and without Source-Destination Link for the Case of Quantized Phase Shifts in  $\kappa$ - $\mu$  Fading,” *IEEE Transactions on Communications*, 2021.
- [20] Q.-U.-A. Nadeem, A. Kammoun, A. Chaaban, M. Debbah, and M.-S. Alouini, “Asymptotic Max-Min SINR Analysis of Reconfigurable Intelligent Surface Assisted MISO Systems,” *IEEE Transactions on Wireless Communications*, vol. 19, no. 12, pp. 7748–7764, 2020.
- [21] A. Abrardo, D. Dardari, and M. Di Renzo, “Intelligent reflecting surfaces: Sum-rate optimization based on statistical CSI,” *arXiv preprint arXiv:2012.10679*, 2020.
- [22] A. Subhash, A. Kammoun, A. Elzanaty, S. Kalyani, Y. H. Al-Badarneh, and M.-S. Alouini, “Max-Min SINR Optimization for RIS-aided Uplink Communications with Green Constraints,” *ArXiv*, 2022.
- [23] L. Chiaraviglio, A. Elzanaty, and M.-S. Alouini, “Health risks associated with 5G exposure: A view from the communications engineering perspective,” *IEEE Open Journal of the Communications Society*, vol. 2, pp. 2131–2179, 2021.
- [24] Y. A. Sambo, F. Heliot, and M. A. Imran, “A survey and tutorial of electromagnetic radiation and reduction in mobile communication systems,” *IEEE Communications Surveys & Tutorials*, vol. 17, no. 2, pp. 790–802, 2014.
- [25] M. Wang, L. Lin, J. Chen, D. Jackson, W. Kainz, Y. Qi, and P. Jarmuszewski, “Evaluation and optimization of the specific absorption rate for multiantenna systems,” *IEEE transactions on electromagnetic compatibility*, vol. 53, no. 3, pp. 628–637, 2011.
- [26] A. Elzanaty, L. Chiaraviglio, and M.-S. Alouini, “5G and EMF Exposure: Misinformation, Open Questions, and Potential Solutions,” *Frontiers in Communications and Networks*, vol. 2, 2021. [Online]. Available: <https://www.frontiersin.org/articles/10.3389/frcmn.2021.635716>
- [27] H. Ibraiwish, A. Elzanaty, Y. H. Al-Badarneh, and M.-S. Alouini, “EMF-aware cellular networks in RIS-assisted environments,” *IEEE Communications Letters*, vol. 26, no. 1, pp. 123–127, 2021.
- [28] D. S. Javed, A. Elzanaty, O. Amin, M.-S. Alouini, and B. Shihada, “EMF-Aware Probabilistic Shaping Design for Hardware Distorted Communication Systems,” *Frontiers in Communications and Networks*, p. 13.

- [29] F. Héliot and T. W. C. Brown, “On the Exposure Dose Minimization of Multi-Antenna Multi-Carrier System Users,” *IEEE Transactions on Vehicular Technology*, vol. 71, no. 7, pp. 7625–7638, 2022.
- [30] D. W. Cai, T. Q. Quek, and C. W. Tan, “A unified analysis of max-min weighted SINR for MIMO downlink system,” *IEEE Transactions on Signal Processing*, vol. 59, no. 8, pp. 3850–3862, 2011.
- [31] M. Grant and S. Boyd, “CVX: Matlab Software for Disciplined Convex Programming, version 2.1,” <http://cvxr.com/cvx>, Mar. 2014.
- [32] C. W. Tan, “Wireless network optimization by Perron-Frobenius theory,” in *2014 48th Annual Conference on Information Sciences and Systems (CISS)*. IEEE, 2014, pp. 1–6.
- [33] “Further Advancements for E-UTRA Physical Layer Aspects,” 3GPP, TR 36.814, March 2010, version 9.0.0.
- [34] A. Kammoun and M.-S. Alouini, “On the precise error analysis of support vector machines,” *IEEE Open Journal of Signal Processing*, vol. 2, pp. 99–118, 2021.